Hyaluronate–Gold Nanoparticle/Tocilizumab Complex for the Treatment of Rheumatoid Arthritis

Hwiwon Lee,[†] Min-Young Lee,[†] Suk Ho Bhang,[‡] Byung-Soo Kim,[‡] Yun Seop Kim,[†] Ji Hyeon Ju,[§] Ki Su Kim,[⊥] and Sei Kwang Hahn[†,*]

[†]Department of Materials Science and Engineering, Pohang University of Science and Technology (POSTECH), 77 Cheongam-ro, Nam-gu, Pohang, Kyungbuk 790-784, Korea, [‡]School of Chemical and Biological Engineering, Seoul National University, San 56-1, Sillim-dong, Gwanak-gu, Seoul 151-744, Korea, [§]Department of Internal Medicine, College of Medicine, The Catholic University of Korea, 505 Banpo-dong, Seocho-gu, Seoul 137-701, Korea, and [⊥]Wellman Center for Photomedicine, Harvard Medical School and Massachusetts General Hospital, 65 Landsdowne Street UP-5, Cambridge, Massachusetts 02139, United States

ABSTRACT Rheumatoid arthritis (RA) is a chronic inflammatory immune disease causing the inflammation of synovial membrane and the articular cartilage destruction. In this work, hyaluronate–gold nanoparticle/Tocilizumab (HA-AuNP/TCZ) complex was prepared for the treatment of RA. AuNP was used as a drug carrier with antiangiogenic effect. TCZ is a humanized monoclonal antibody against the interleukin-6 (IL-6) receptor and used as an immunosuppressive drug by interfering IL-6 in the pathogenesis of RA. HA is known to have cartilage-protective and lubricant effects. HA was modified with cystamine *via* reductive amination, which was reduced with dithiothreitol (DTT) to prepare end-group thiolated HA (HA-SH). AuNP was chemically modified with HA-SH and physically modified with TCZ. The formation of HA-AuNP/TCZ complex was corroborated by UV–vis spectroscopy, dynamic light scattering (DLS), and transmission electron microscopy (TEM). The therapeutic effect of HA-AuNP/TCZ complex on RA was confirmed in collagen-induced arthritis (CIA) model mice by ELISA, histological, and Western blot analyses.

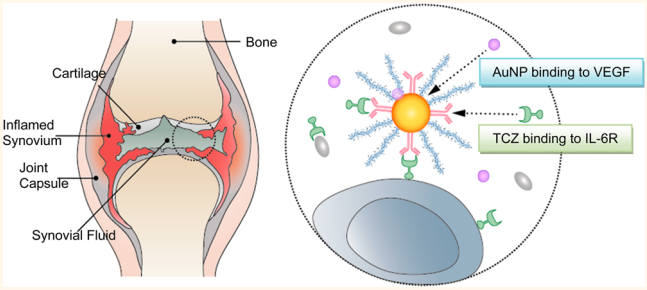

KEYWORDS: gold nanoparticle · tocilizumab · hyaluronic acid · drug delivery · rheumatoid arthritis

Gold nanoparticles (AuNPs) have been widely used for various biomedical applications because of their biocompatibility, simple synthesis, facile surface modification, versatile conjugation with biomolecules, and tunable optical properties.[1−5] Moreover, AuNPs are known to have an antiangiogenic effect[6] by binding vascular endothelial growth factor (VEGF),[7] which plays a crucial role in the pathogenesis of rheumatoid arthritis (RA).[8,9] Recent studies have shown that AuNPs are a potential antioxidant.[10] By quenching reactive oxygen species (ROS), AuNPs inhibit the receptor activator of nuclear factor−κB ligand (RANKL)-induced osteoclast formation, which results in the bone and cartilage erosion.[10] Since VEGF, osteoclast, and ROS are the main contributors to the pathogenesis of RA, AuNPs have been considered as a therapeutic agent for the treatment of RA. Furthermore, because of its optical properties,[11,12] AuNPs can be used as a nanoprobe and contrast agent for selectively detecting a target molecule and diagnosing the progress of RA.[13,14]

RA is a chronic inflammatory autoimmune disease that results in long-standing synovitis, bone destruction, and finally joint dysfunction. Proinflammatory cytokines such as tumor necrosis factor alpha (TNFα), interleukin 6 (IL-6), and VEGF play an important role for aggravation and sustainability of joint inflammation.[9,15] TNFα inhibitors have shown the therapeutic effect on the intractable RA,[16] opening a new era for biological drugs of monoclonal antibodies[17] and Fc-fusion proteins.[18] Among prevailing biological drugs, IL-6 is the second most popular cytokine target of biopharmaceuticals. IL-6 is a pleiotropic cytokine that is overexpressed in synovial tissues of RA patients with increased concentrations in serum and synovial fluid.[19,20] IL-6 affects the function of neutrophils, T cells, B cells, monocytes, and osteoclasts,

* Address correspondence to skhanb@postech.ac.kr.

Received for review February 4, 2014 and accepted April 9, 2014.

Published online April 14, 2014
10.1021/nn500685h

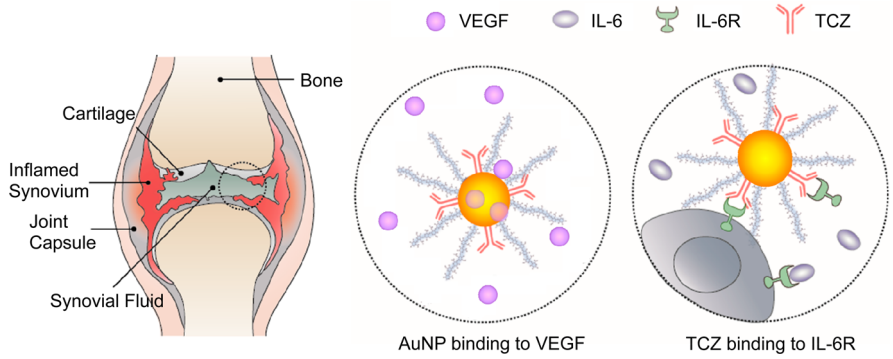

Figure 1. Schematic illustration of HA-AuNP/TCZ complex for the treatment of RA by the dual targeting to VEGF and IL-6R.

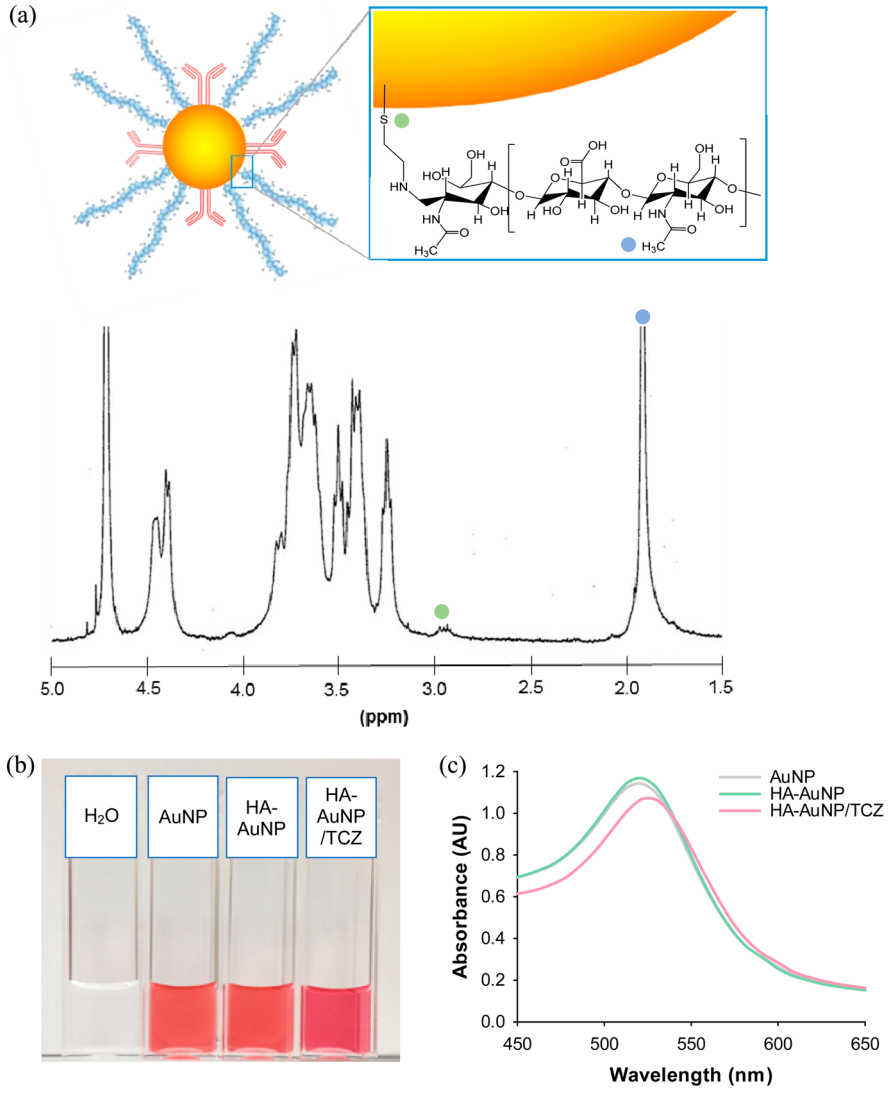

Figure 2. (a) ^{1}H NMR of end group thiolated HA in HA-AuNP/TCZ complex. (b) Photographic images of H_2O, and the solutions of AuNP, HA-AuNP, and HA-AuNP/TCZ complex. (c) UV−vis spectra of AuNP, HA-AuNP, and HA-AuNP/TCZ complex.

which are highly activated in RA patients. IL-6 is the major inducer of the hepatic acute phase response, a key feature of RA.[21] Tocilizumab (TCZ) is the first monoclonal therapeutic antibody against IL-6 signaling by binding IL-6 receptor (IL-6R), which finally antagonizes the interaction of IL-6 with IL-6R.[22] TCZ has gained its popularity for rapidly suppressing inflammation and preventing joint destruction.[23] Nowadays, the second generation biopharmaceuticals are intensively investigated to potentiate the former biological drugs by changing chemical structures and properties.[24,25]

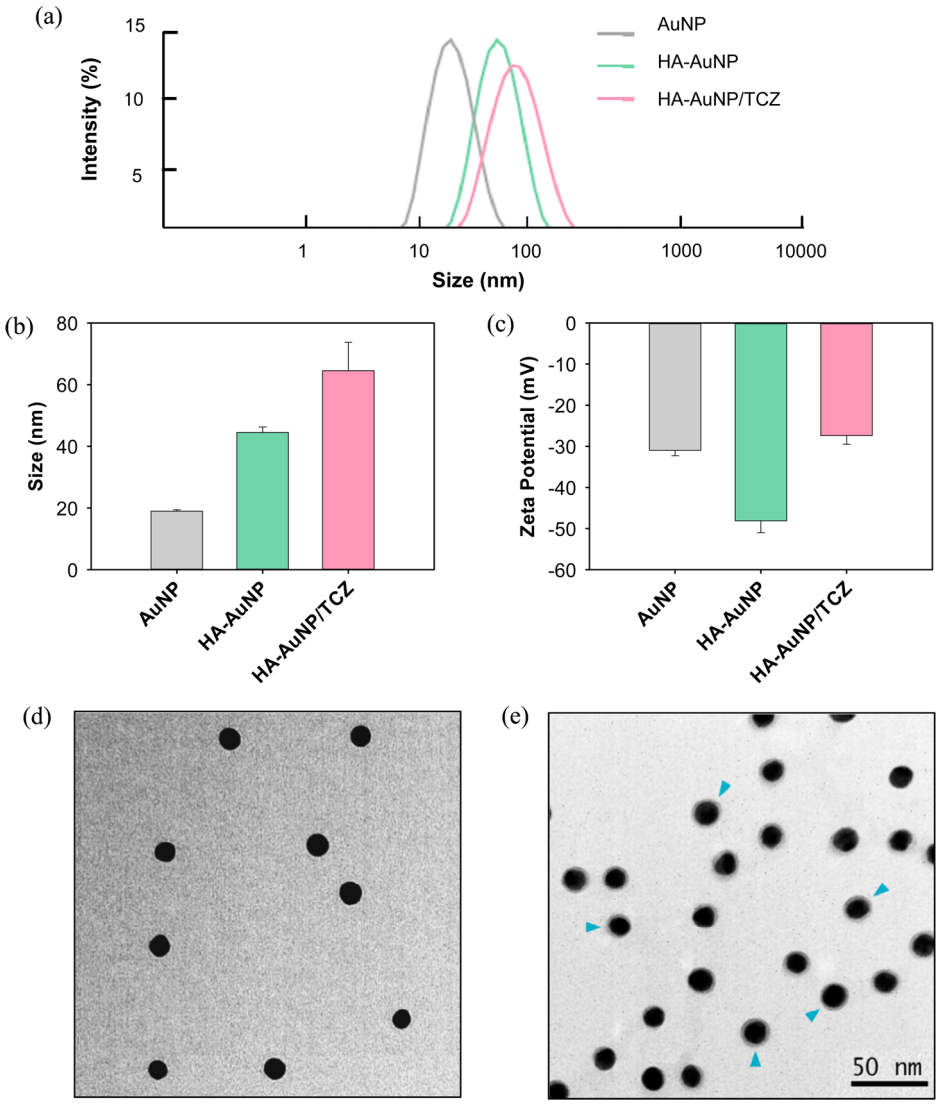

Figure 3. (a,b) The hydrodynamic diameters and (c) zeta potentials of AuNP, HA-AuNP, and HA-AuNP/TCZ complex (n = 3). TEM images of (d) HA-AuNP and (e) HA-AuNP/TCZ complex.

In this work, we developed a new RA treatment system using hyaluronate (HA)−AuNP/TCZ complex. As well as biocompatible, biodegradable, nonimmunogenic, and nontoxic characteristics, HA has unique rheological property, showing cartilage protective and lubricant effects in synovial fluid.[26,27] Moreover, the stability of HA-AuNP/TCZ complex can be drastically improved by the HA on the surface, reducing its nonspecific binding to serum proteins in the body.[4] RA pathogenesis, where many types of proinflammatory cytokines and immunocytes are working together, is so complicated that completely alleviating the events of RA is very difficult by using one interfering molecule. In contrast, HA-AuNP/TCZ complex can have its synergistic effect on RA by simultaneously targeting VEGF and IL-6R. After *in vitro* characterization, we assessed the therapeutic efficacy of HA-AuNP/TCZ complex for the treatment of RA and discussed the feasibility for further clinical applications.

RESULTS AND DISCUSSION

Preparation and Characterization of HA-AuNP/TCZ Complex. The combination therapy of RA has been widely investigated with multiple interfering molecules.[28] As schematically illustrated in Figure 1, we prepared a dual targeting HA-AuNP/TCZ complex that can simultaneously bind to VEGF and IL-6R for the treatment of RA. AuNP is used as a drug carrier and binds to VEGF showing antiangiogenic effect on RA. TCZ is an immunosuppressive drug interfering IL-6 in the pathogenesis of RA. HA is widely used for cartilage-protection and lubrication. For the preparation of the complex, HA was modified with cystamine *via* reductive amination to synthesize end-group thiolated HA (HA-SH). AuNPs were prepared by reducing and stabilizing $HAuCl_4$ with sodium citrate in boiling condition as we reported elsewhere.[4] After that, AuNPs were chemically modified with HA-SH *via* the gold−thiol chemistry[29,30] and physically modified with TCZ *via*

hydrophobic and electrostatic interactions.[4] The remaining unbound HA-SH and TCZ were removed by centrifugation and resuspension three times. The successful formation of HA-AuNP/TCZ complex was confirmed by UV−vis spectroscopy, dynamic light scattering (DLS), and transmission electron microscopy (TEM) as described in the following section.

Figure 2a shows ^{1}H NMR analysis of HA-SH. According to the Ellman's assay, more than 90% of HA was end thiol modified. From the results, we could confirm the successful synthesis of HA-SH. Figure 2b shows the UV−vis spectroscopy reflecting the formation of HA-AuNP/TCZ complex. The strong interaction of AuNP with HA-SH and TCZ was corroborated from the red shift in the surface plasmon resonance (SPR) peak (Figure 2c). The SPR peak of free AuNP appeared around 521 nm, and the stepwise binding of HA-SH and TCZ to AuNP shifted the SPR peak to 523 and 525 nm, respectively. The hydrodynamic size and the surface charge of the complex were analyzed by DLS (Figure 3a, 3b). The hydrodynamic size of AuNP was *ca.* 19.02 nm with a narrow PDI of 0.18 and that of HA-AuNP was *ca.* 46.54 nm with a PDI of 0.17. The diameter of HA-AuNP/TCZ complex was *ca.* 64.83 nm with a PDI of 0.18. The surface charge of AuNP, HA-AuNP, and HA-AuNP/TCZ complex was changed with the values of −30.35 ± 2.05 mV, −46.65 ± 4.35 mV, and −25.65 ± 3.65 mV, respectively (Figure 3c). Furthermore, the monodisperse formation of the HA-AuNP/TCZ complex was also confirmed by TEM. The size of AuNP was *ca.* 15 nm, and the layer of TCZ surrounding AuNP was observed on the TEM image (Figure 3d,e). The content of HA and TCZ bound to a single AuNP was determined by measuring the absorbance of HiLyte-labeled HA and TCZ, which revealed that *ca.* 41.99 of HA and *ca.* 20.82 of TCZs were bound to the single AuNP. The stability of HA-AuNP/TCZ complex was assessed in BSA solution (10 mg/mL) and heparin solution (1 mg/mL) for 8 days. While AuNPs rapidly aggregated in both BSA and heparin solutions, HA-AuNP/TCZ complexes remained stable for more than a week. TCZ was steadily released from the HA-AuNP/TCZ complex up to *ca.* 80% for 8 days after incubation in the BSA solution, reflecting the feasibility for *in vivo* applications to RA. In case of heparin solution, only *ca.* 10% of TCZ was released from the complex.

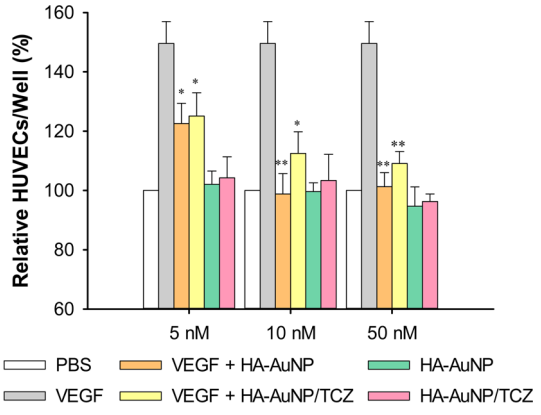

Figure 4. Effect of AuNPs (5, 10, and 50 nM) on the VEGF (10 ng/mL) induced proliferation of HUVECs. The values of **P < 0.01 and *P < 0.05 in comparison with the VEGF treated group were considered to be statistically significant (n = 4).

***In Vitro* Biological Activity of HA-AuNP/TCZ Complex.** AuNP is known to inhibit VEGF-induced proliferation of human umbilical vein endothelial cells (HUVECs). To assess the antiangiogenic effect of HA-AuNP/TCZ complex, MTT assay of HUVECs treated with VEGF (10 ng/mL) was performed with increasing concentration of AuNP from 5 to 50 nM (Figure 4). The treatment with VEGF resulted in the accelerated proliferation of HUVECs more than 150% of the control group. The proliferation of HUVECs was not changed in the presence of HA-AuNP or HA-AuNP/TCZ complex. However, after preincubation with HA-AuNP or HA-AuNP/TCZ complex, the proliferation of HUVECs in the presence of VEGF decreased to the statistically significant levels. Especially, when the concentration of AuNP changed from 5 to 10 nM, the VEGF-induced HUVEC proliferation decreased drastically. There was little difference in the proliferation between 10 and 50 nM of AuNPs, reflecting the saturated binding of AuNP with VEGF at a concentration around 10 nM. The results clearly

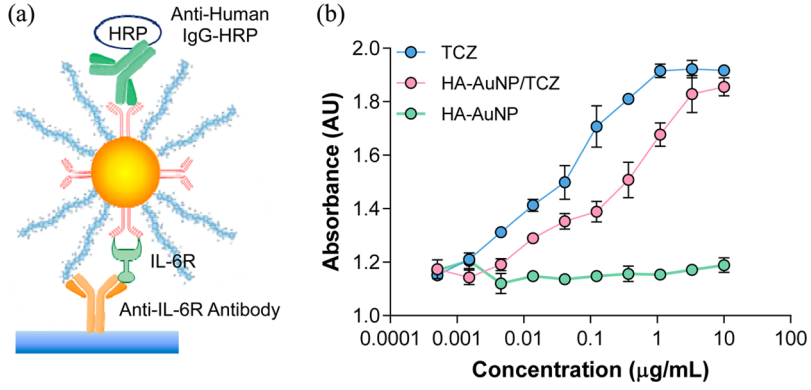

Figure 5. (a) Schematic illustration for the binding test of HA-AuNP/TCZ complex to IL-6R by ELISA and (b) the results for the binding of TCZ and HA-AuNP/TCZ complex to IL-6R (n = 3).

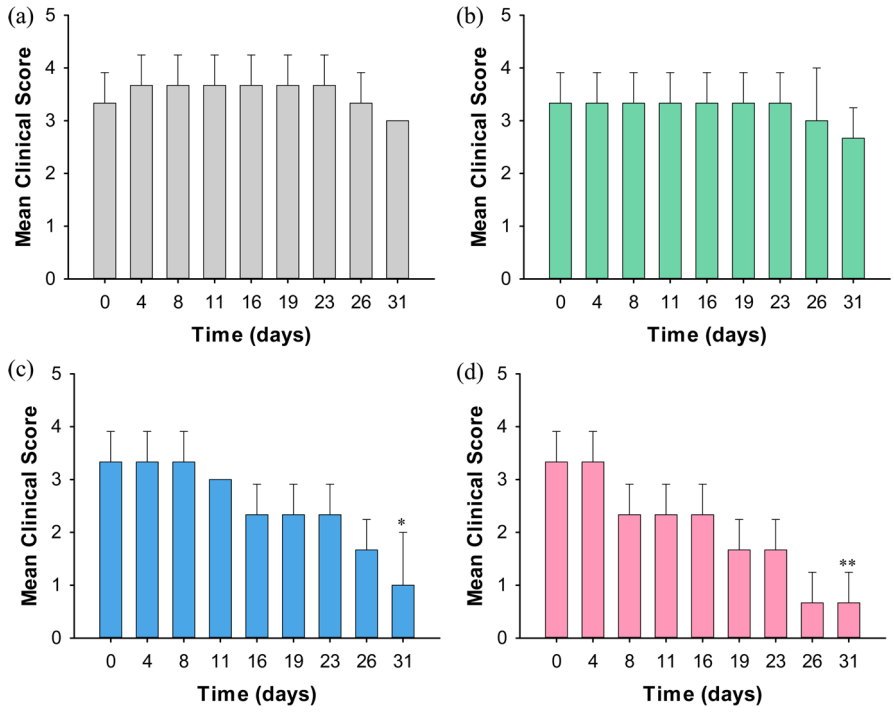

Figure 6. Mean clinical scores for the paws of collagen-induced arthritis DBA/1j mice after treatments with (a) PBS, (b) HA-AuNP, (c) TCZ, and (d) HA-AuNP/TCZ complex ($P < 0.01$ and *$P < 0.05$ in comparison with the group at 0 day, $n = 3$).**

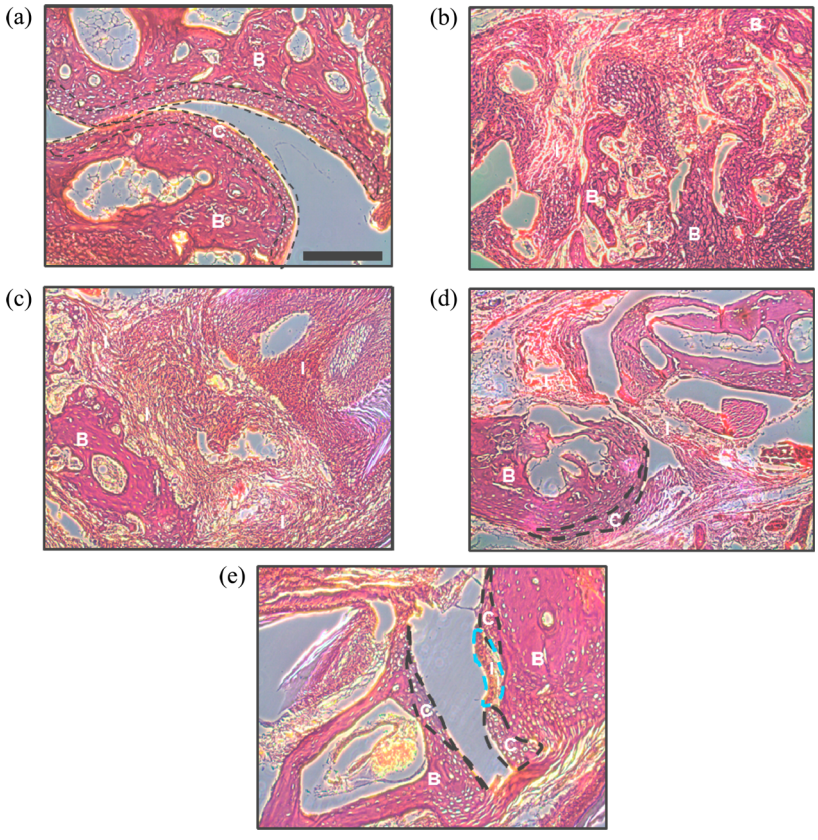

Figure 7. Histological analysis with H&E staining of dissected joint tissues in 4 weeks: (a) the control of normal DBA/1j mouse, (b) the negative control of collagen-induced arthritis DBA/1j mouse treated with PBS, those treated with (c) HA-AuNP, (d) TCZ, and (e) HA-AuNP/TCZ complex. Scale bar indicates 150 μm (B = bone, C = cartilage, I = inflammation).

showed the antiangiogenic effect of HA-AuNP/TCZ complex on the proliferation of HUVECs by binding to VEGF. The biological activity of HA-AuNP/TCZ complex was further confirmed by ELISA for the binding of

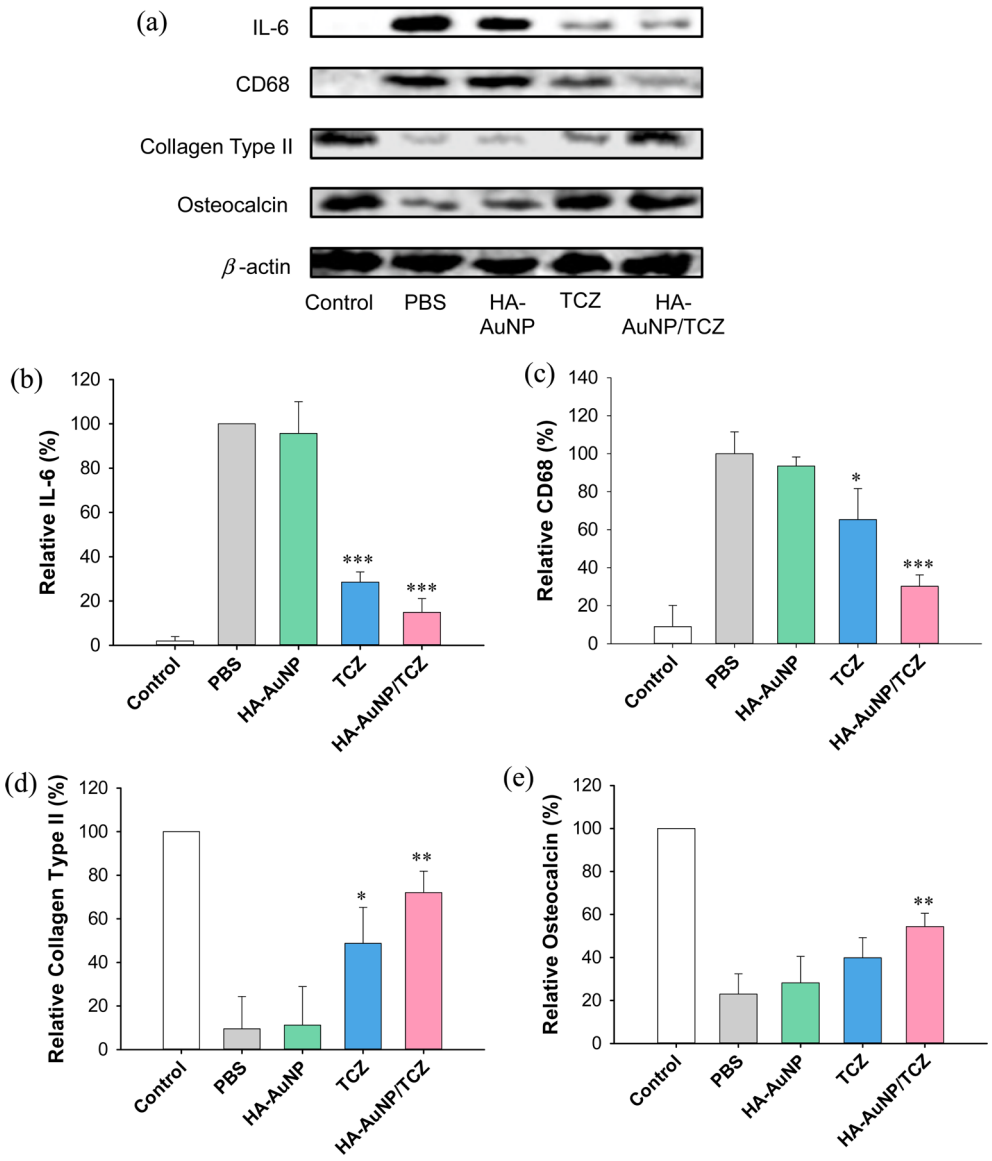

Figure 8. (a) Western blot analysis of IL-6, CD68, collagen type II, and osteocalcin in the dissected joint tissues in 4 weeks for the cases of the control of normal DBA/1j mouse, the negative control of collagen-induced arthritis DBA/1j mouse treated with PBS, those treated with HA-AuNP, TCZ, and HA-AuNP/TCZ complex. Densitometric analysis of the Western blot bands of (b) IL-6, (c) CD68, (d) Collagen type II, and (e) Osteocalcin (*$P < 0.0001$, **$P < 0.01$, and *$P < 0.05$ in comparison with PBS treated group, $n = 3$).**

HA-AuNP/TCZ complex to IL-6R (Figure 5). The binding of HA-AuNP/TCZ complex was significantly enhanced with increasing concentration of TCZ, which was slightly lower than that of TCZ alone, likely due to the steric hindrance of HA in the complex. From the results, we could confirm the dual binding affinity of HA-AuNP/TCZ complex to VEGF and IL-6R.

***In Vivo* Efficacy of HA-AuNP/TCZ Complex in RA Model Mice.** Collagen-induced arthritis (CIA) animal models ($n = 3$) were treated at one arthritic ankle joint per animal with four types of samples (15 μL): PBS for group 1, HA-AuNP for group 2, TCZ for group 3, and HA-AuNP/TCZ complex for group 4. The swelling of joints was observed twice a week after sample injection. Figure 6 shows the mean clinical scores[31] of arthritic paws treated with the samples. Although the HA-AuNP treatment in group 2 showed a slight improvement in the mean clinical scores with increasing time, there was not so much big difference between groups 1 and 2 (Figure 6a,b). However, groups 3 and 4 showed obvious improvement in the degree of swelling (Figure 6c,d). Remarkably, the mean clinical score in group 4 was statistically better than that in group 2. The results indicate that HA-AuNP/TCZ complex has a better therapeutic effect than those of TCZ as well as HA-AuNP, possibly because of the long-term synergistic dual effect of HA-AuNP/TCZ complex.

The therapeutic effect of HA-AuNP/TCZ complex was further investigated on the inflammation and the destruction level of cartilage and bone by the

histological analysis with hematoxylin and eosin (H&E) staining. Normal mice without RA induction showed no signs of inflammation and no destruction of cartilage and bone (Figure 7a). The interface between cartilage and bone in the tissues were clearly distinguished by their morphologies. However, RA model mice in group 1 treated with PBS showed severe inflammation and the cartilage and bone destruction (Figure 7b). The interface between cartilage and bone was hard to distinguish by inflammatory cell infiltration and the cartilage and bone destruction. While the treatment with HA-AuNP showed no significant therapeutic effect (Figure 7c), groups 3 and 4 showed considerably reduced levels of inflammatory cell infiltration and cartilage and bone destruction (Figures 7d,e). Especially, the treatment with HA-AuNP/TCZ complex in group 4 resulted in the clear interface between cartilage and bone comparable to the normal control group (Figure 7e). Remarkably, in contrast to the synovial hypertrophy with cellular infiltration in TCZ treatment group (Figure 7d), it was not observed in the treatment group with HA-AuNP/TCZ complex (Figure 7e).

Western blot analysis also confirmed the therapeutic effect of HA-AuNP/TCZ complex (Figure 8). While the negative control group showed significantly upregulated expression levels of IL-6 and CD68, the treatment with HA-AuNP/TCZ complex resulted in significantly reduced levels of IL-6 and CD68 (Figure 8a–c). CD68 is the marker for the various cells of the macrophage lineage. In addition, the expression level of collagen type II and osteocalcin was greatly increased by the treatment with HA-AuNP/TCZ complex (Figure 8a,d,e). Taken together, we could confirm the therapeutic effect of HA-AuNP/TCZ complex for the treatment of RA by dual targeting to VEGF and IL-6R. As we previously reported elsewhere,[4] the novel HA-AuNP/protein complex can be used as a platform delivery carrier of various protein therapeutics.

CONCLUSION

HA-AuNP/TCZ complex was successfully prepared for the treatment of RA. The formation of HA-AuNP/TCZ complex was clearly confirmed by UV–vis spectroscopy, DLS, and TEM analysis. *In vitro* biological activity of dual targeting HA-AuNP/TCZ complex was confirmed for the binding to VEGF and IL-6R. The therapeutic effect of HA-AuNP/TCZ complex on RA in model mice was verified by ELISA, histological, and Western blot analyses. Taken together, HA-AuNP/TCZ complex might be developed as a dual targeting drug candidate to VEGF and IL-6R for the treatment of RA. Furthermore, the novel platform of HA-AuNP/protein complex can be used for various therapeutic applications.

MATERIALS AND METHODS

Materials. Chloroauric acid ($HAuCl_4$), sodium citrate, sodium cyanoborohydride ($NaBH_3CN$), and histological decalcifying solution were obtained from Sigma-Aldrich (St. Louis, MO). Sodium hyaluronate with a molecular weight of 17 kDa was purchased from Lifecore Co. (Chaska, MN). Cystamine dihydrochloride was purchased from Tokyo Chemical Industry (Tokyo, Japan). HiLyte 647 amine and HiLyte 647 succinimidyl ester were purchased from AnaSpec Inc. (Fremont, CA). Recombinant human VEGF165 was purchased from BioLegend (San Diego, CA). Endothelial cell growth media kits (EGM-2 Bulletkit) were purchased from Lonza (Walkersville, MD). HUVECs were obtained from InnoPharmaScreen, Inc. (Asan, Korea). Human IL-6Rα antibody, recombinant human IL-6Rα, and recombinant human IL-6 were purchased from R&D systems (Minneapolis, MN). Anti-IL-6 antibody (HRP) and primary antibodies against IL-6, CD68, collagen type II, and osteocalcin were obtained from Abcam (Cambridge, MA). Goat antihuman IgG-HRP was purchased from Santa Cruz Biotechnology (Santa Cruz, CA). Tocilizumab (TCZ) was obtained from JW Pharmaceutical (Seoul, Korea). We have complied with the POSTECH institutional ethical protocols for animals.

Preparation of HA-AuNP/TCZ Complex. AuNPs were synthesized using citrate as a reducing agent and stabilizer. $HAuCl_4$ (10 mg) was dissolved in boiling water (90 mL) and mixed with sodium citrate solution (73.515 mg/mL, 0.25 mL), which stirred until the color of solution turned wine-red. The reaction solution was incubated for 1 day and filtered with a PVDF syringe filter (0.45 μm). For the synthesis of HA-AuNP conjugate, end group thiolated HA (HA-SH) was synthesized by reductive amination as we described elsewhere.[4] The HA-SH solution (5 mg/mL, 0.004 mL) was added to the AuNP solution (1 mL), which stirred for 4 h. HA-AuNP was purified by the successive steps of centrifugation (25000*g*, 25 min) and redispersion in DI water. Then, 0.2 mL of TCZ solution (0.1 mg/mL) in PBS was added to 1 mL of the HA-AuNP solution. After incubation at room temperature with mild stirring for 4 h, HA-AuNP/TCZ complex was purified by centrifugation and finally redispersed in PBS.

Characterization of HA-AuNP/TCZ Complex. The formation of HA-AuNP/TCZ complex was analyzed with a UV–vis spectrophotometer (S-3100, Scinco Co., Seoul, Korea). The hydrodynamic size and zeta potential of HA-AuNP/TCZ complex were measured by DLS (n = 3, Zetasizer Nano, Malvern Instrument Co., UK). The formation of the HA-AuNP/TCZ complex was also analyzed by TEM operating at 300 kV. The average number of HA and TCZ bound to the single AuNP was determined by measuring the fluorescence intensity of HiLyte-labeled HA and TCZ after etching the AuNP in KCN to avoid the quenching of the dye.[13] The fluorescence of HiLyte was detected with a spectrofluorophotometer at the excitation/emission wavelength of 584/650 nm. *In vitro* release tests of TCZ from HA-AuNP/TCZ complex were performed using HiLyte-labeled TCZ. HA-AuNP/HiLyte-TCZ complex was incubated in BSA solution (10 mg/mL) or heparin solution (1 mg/mL) in a shaking incubator at 37 °C for 8 days. After centrifugation of HA-AuNP/TCZ complex, the supernatant was removed, and AuNPs were etched with KCN. The remaining amount of HiLyte-TCZ was determined by detecting at the excitation/emission wavelength for the HiLyte.

***In Vitro* Assessment for Antiangiogenic Effect of HA-AuNP/TCZ Complex.** The antiangiogenic effect of HA-AuNP/TCZ complex was assessed by MTT assay for the inhibition of VEGF-induced proliferation of HUVECs.[7] First, 1×10^4 HUVECs/well were seeded in 96-well plates, cultured in EGM for 1 day, and then incubated in EBM with 0.2% of FBS overnight. After that, VEGF (10 ng/mL) was mixed with HA-AuNP/TCZ complex (5, 10, or 50 nM of AuNP) at 4 °C overnight, which was added to the serum starved HUVECs. HUVECs were incubated in a humidified 5% CO_2 incubator at 37 °C for 24 h. The cells were washed with PBS and incubated in the mixed solution of serum free EBM (100 μL) and MTT solution

(10 μL, 5 mg/mL) in the well for 2 h. The mixed solution of EBM and MTT was removed, and 50 μL of DMSO was added to each well. Optical densities were measured at 540 nm with a microplate reader (EMax, Molecular Devices, CA).

***In Vitro* Binding Affinity Tests of HA-AuNP/TCZ Complex to IL-6R.** The biological activity of HA-AuNP/TCZ complex for the binding to IL-6R was assessed by ELISA.[32] First, anti-IL-6R antibody at a concentration of 4 μg/mL in a coating buffer was incubated in a 96-well plate at 4 °C overnight for the preparation of anti-IL-6R antibody coated wells. After washing with TTBS buffer, the wells were blocked with a blocking buffer at room temperature for 2 h. Then, 100 μL of recombinant human IL-6Rα (2 μg/mL) was added to the well and incubated for 2 h. After washing, various concentrations from 0.0005 to 10 μg/mL of TCZ or HA-AuNP/TCZ complex were added to the wells and incubated at room temperature for 2 h. After washing again, goat antihuman IgG-HRP was incubated for 2 h, and the supernatant in the wells was removed. Finally, 50 μL of TMB solution was added to the well. After 30 min incubation, the stop solution was added. The absorbance was measured at 450 nm with the microplate reader.

***In Vivo* Assessment for the Therapeutic Effect of HA-AuNP/TCZ Complex.** Collagen-induced arthritis (CIA) animal models were prepared using DBA/1j mice.[31] DBA/1j mice were immunized with collagen emulsified in Complete Freund's Adjuvant (CFA), followed by the boosting injection of collagen emulsified in Incomplete Freund's Adjuvant (IFA). In detail, 50 μL of the mixed solution of CFA (1.0 mg/mL) and type II collagen (2.0 mg/mL) at a volume ratio of 1:1 was intradermally injected into the tail. A booster injection was performed 21 days after the initial immunization with 50 μL of the mixed solution of IFA (1.0 mg/mL) and type II collagen (2.0 mg/mL) at a volume ratio of 1:1. The emulsion was again intradermally injected into the proximal tail. The mice were monitored two to three times in a week after the first immunization. Each paw was evaluated and scored individually at a scale of 0−4 depending on the evidence of erythema and swelling. The score 0 is for a normal paw and the score 1 for erythema and weak swelling limited to one toe. The score 2 is for erythema and weak swelling on more than one toe but not entire paw. The score is 3 when erythema and moderate swelling are extending to entire paw. The score 4 indicates the most severe erythema and swelling for the whole paw and ankle or ankylosed paw. The RA model mice ($n = 3$) were treated at one arthritic ankle joint per mouse with four types of samples at 5 weeks after initial immunization: PBS for group 1, HA-AuNP for group 2, TCZ for group 3, and HA-AuNP/TCZ complex for group 4. The final volume of each sample was 15 μL containing the equal amount of TCZ (0.8 mg/kg). The treated mice were monitored and scored by three blinded experimenters to assess the therapeutic effect of the samples on RA for a month and then sacrificed for the following histological and Western blot analyses.

Histological Analysis. All specimens were fixed in 10% (v/v) buffered formalin and decalcified with a histological decalcifying solution for 7 days. After decalcification, samples were washed with DI water five times, dehydrated again with a graded ethanol series, and embedded in paraffin. Tissues were sliced into 4 μm-thick sections. The tissue sections were stained with H&E. The images of sections were obtained with a light microscope (Model IX71 Olympus, Tokyo, Japan).

Western Blot Analysis. The inflammation, cartilage and bone degeneration of samples were evaluated by the detection of the protein marker in the Western blot analysis. Tissue samples were washed three times with PBS and lysed by the addition of SDS sample buffer containing 62.5 mM Tris−HCl (pH 6.8), 2% SDS, 10% glycerol, 50 mM dithiothreitol, and 0.1% bromophenol blue. Extracted proteins were electrophoretically separated on 4−10% SDS polyacrylamide gels and transferred to membranes. For the protein detection, membranes were incubated with primary antibodies against IL-6, CD68, collagen type II, and osteocalcin at 4 °C overnight, washed, and incubated with secondary antibodies conjugated to horseradish peroxidase at room temperature for 50 min. Blots were developed using enhanced chemiluminescence. The luminescence was recorded on X-ray film (Fuji super RX, Fujifilm Medical Systems, Tokyo, Japan), and the bands were imaged and quantified with an Imaging Densitometer (Bio-Rad, Hercules, CA).

Conflict of Interest: The authors declare no competing financial interest.

Acknowledgment. This work was supported by the Converging Research Center Program through the National Research Foundation of Korea (NRF) funded by the Ministry of Education, Science and Technology (2009-0081871). This study was also supported by Midcareer Researcher Program through NRF grant funded by the MEST (No. 2012R1A2A2A06045773).

REFERENCES AND NOTES

1. Ghosh, P.; Han, G.; De, M.; Kim, C. K.; Rotello, V. M. Gold Nanoparticles in Delivery Applications. *Adv. Drug Delivery Rev.* **2008**, *60*, 1307–1315.
2. Thakor, A. S.; Jokerst, J.; Zavaleta, C.; Massoud, T. F.; Gambhir, S. S. Gold Nanoparticles: A Revival in Precious Metal Administration to Patients. *Nano Lett.* **2011**, *11*, 4029–4036.
3. Giljohann, D. A.; Seferos, D. S.; Daniel, W. L.; Massich, M. D.; Patel, P. C.; Mirkin, C. A. Gold Nanoparticles for Biology and Medicine. *Angew. Chem., Int. Ed.* **2010**, *49*, 3280–3294.
4. Lee, M. Y.; Yang, J. A.; Jung, H. S.; Beack, S.; Choi, J. E.; Hur, W.; Koo, H.; Kim, K.; Yoon, S. K.; Hahn, S. K. Hyaluronic Acid-Gold Nanoparticle/Interferon Alpha Complex for Targeted Treatment of Hepatitis C Virus Infection. *ACS Nano* **2012**, *6*, 9522–9531.
5. Lee, M. Y.; Park, S. J.; Park, K.; Kim, K. S.; Lee, H.; Hahn, S. K. Target-Specific Gene Silencing of Layer-by-Layer Assembled Gold-Cysteamine/siRNA/PEI/HA Nanocomplex. *ACS Nano* **2011**, *5*, 6138–6147.
6. Mukherjee, P.; Bhattacharya, R.; Wang, P.; Wang, L.; Basu, S.; Nagy, J. A.; Atala, A.; Mukhopadhyay, D.; Soker, S. Antiangiogenic Properties of Gold Nanoparticles. *Clin. Cancer Res.* **2005**, *11*, 3530–3534.
7. Bhattacharya, R.; Mukherjee, P.; Xiong, Z.; Atala, A.; Soker, S.; Mukhopadhyay, D. Gold Nanoparticles Inhibit VEGF165-Induced Proliferation of HUVEC Cells. *Nano Lett.* **2004**, *4*, 2479–2481.
8. Tsai, C. Y.; Shiau, A. L.; Chen, S. Y.; Chen, Y. H.; Cheng, P. C.; Chang, M. Y.; Chen, D. H.; Chou, C. H.; Wang, C. R.; Wu, C. L. Amelioration of Collagen-Induced Arthritis in Rats by Nanogold. *Arthritis Rheum.* **2007**, *56*, 544–554.
9. Firestein, G. S. Evolving Concepts of Rheumatoid Arthritis. *Nature* **2003**, *423*, 356–361.
10. Sul, O. J.; Kim, J. C.; Kyung, T. W.; Kim, H. J.; Kim, Y. Y.; Kim, S. H.; Kim, J. S.; Choi, H. S. Gold Nanoparticles Inhibited the Receptor Activator of Nuclear Factor-Kappab Ligand (RANKL)-Induced Osteoclast Formation by Acting as an Antioxidant. *Biosci. Biotechnol. Biochem.* **2010**, *74*, 2209–2213.
11. Jain, P. K.; Lee, K. S.; El-Sayed, I. H.; El-Sayed, M. A. Calculated Absorption and Scattering Properties of Gold Nanoparticles of Different Size, Shape, and Composition: Applications in Biological Imaging and Biomedicine. *J. Phys. Chem. B* **2006**, *110*, 7238–7248.
12. Chamberland, D. L.; Agarwal, A.; Kotov, N.; Brian Fowlkes, J.; Carson, P. L.; Wang, X. Photoacoustic Tomography of Joints Aided by an Etanercept-Conjugated Gold Nanoparticle Contrast Agent—an *Ex Vivo* Preliminary Rat Study. *Nanotechnology* **2008**, *19*, 095101.
13. Lee, H.; Lee, K.; Kim, I. K.; Park, T. G. Synthesis, Characterization, and *In Vivo* Diagnostic Applications of Hyaluronic Acid Immobilized Gold Nanoprobes. *Biomaterials* **2008**, *29*, 4709–4718.
14. Jeong, E. H.; Jung, G.; Hong, C. A.; Lee, H. Gold Nanoparticle (AuNP)-Based Drug Delivery and Molecular Imaging for Biomedical Applications. *Arch. Pharm. Res.* **2013**, *37*, 53–59.
15. Smolen, J. S.; Aletaha, D.; Koeller, M.; Weisman, M. H.; Emery, P. New Therapies for Treatment of Rheumatoid Arthritis. *Lancet* **2007**, *370*, 1861–1874.
16. Taylor, P. C.; Feldmann, M. Anti-TNF Biologic Agents: Still the Therapy of Choice for Rheumatoid Arthritis. *Nat. Rev. Rheumatol.* **2009**, *5*, 578–582.

17. Olsen, N. J.; Stein, C. M. New Drugs for Rheumatoid Arthritis. *N. Engl. J. Med.* **2004**, *350*, 2167–2179.
18. Huang, C. Receptor-Fc Fusion Therapeutics, Traps, and MIMETIBODY Technology. *Curr. Opin. Biotechnol.* **2009**, *20*, 692–699.
19. Kokkonen, H.; Soderstrom, I.; Rocklov, J.; Hallmans, G.; Lejon, K.; Rantapaa Dahlqvist, S. Up-Regulation of Cytokines and Chemokines Predates the Onset of Rheumatoid Arthritis. *Arthritis Rheum.* **2010**, *62*, 383–391.
20. McInnes, I. B.; Schett, G. The Pathogenesis of Rheumatoid Arthritis. *N. Engl. J. Med.* **2011**, *365*, 2205–2219.
21. Neurath, M. F.; Finotto, S. IL-6 Signaling in Autoimmunity, Chronic Inflammation and Inflammation-Associated Cancer. *Cytokine Growth Factor Rev.* **2011**, *22*, 83–89.
22. Nishimoto, N.; Miyasaka, N.; Yamamoto, K.; Kawai, S.; Takeuchi, T.; Azuma, J.; Kishimoto, T. Study of Active Controlled Tocilizumab Monotherapy for Rheumatoid Arthritis Patients With an Inadequate Response to Methotrexate (SATORI): Significant Reduction in Disease Activity and Serum Vascular Endothelial Growth Factor by IL-6 Receptor Inhibition Therapy. *Mod. Rheumatol.* **2009**, *19*, 12–19.
23. Smolen, J. S.; Beaulieu, A.; Rubbert-Roth, A.; Ramos-Remus, C.; Rovensky, J.; Alecock, E.; Woodworth, T.; Alten, R.; OPTION Investigators. Effect of Interleukin-6 Receptor Inhibition with Tocilizumab in Patients with Rheumatoid Arthritis (OPTION Study): A Double-Blind, Placebo-Controlled, Randomised Trial. *Lancet* **2008**, *371*, 987–997.
24. Leavy, O. Therapeutic Antibodies: Past, Present and Future. *Nat. Rev. Immunol.* **2010**, *10*, 297.
25. Szlachcic, A.; Zakrzewska, M.; Otlewski, J. Longer Action Means Better Drug: Tuning Up Protein Therapeutics. *Biotechnol. Adv.* **2011**, *29*, 436–441.
26. Lo, G. H.; LaValley, M.; McAlindon, T.; Felson, D. T. Intra-Articular Hyaluronic Acid in Treatment of Knee Osteoarthritis: a Meta-Analysis. *JAMA, J. Am. Med. Assoc.* **2003**, *290*, 3115–3121.
27. Kim, K. S.; Park, S. J.; Yang, J. A.; Jeon, J. H.; Bhang, S. H.; Kim, B. S.; Hahn, S. K. Injectable Hyaluronic Acid-Tyramine Hydrogels for the Treatment of Rheumatoid Arthritis. *Acta Biomater.* **2011**, *7*, 666–674.
28. Smolen, J. S.; Steiner, G. Therapeutic Strategies for Rheumatoid Arthritis. *Nat. Rev. Drug Discovery* **2003**, *2*, 473–488.
29. Rouhana, L. L.; Moussallem, M. D.; Schlenoff, J. B. Adsorption of Short-Chain Thiols and Disulfides onto Gold under Defined Mass Transport Conditions: Coverage, Kinetics, and Mechanism. *J. Am. Chem. Soc.* **2011**, *133*, 16080–16091.
30. Hakkinen, H. The Gold-Sulfur Interface at the Nanoscale. *Nat. Chem.* **2012**, *4*, 443–455.
31. Brand, D. D.; Latham, K. A.; Rosloniec, E. F. Collagen-Induced Arthritis. *Nat. Protoc.* **2007**, *2*, 1269–1275.
32. Mihara, M.; Kasutani, K.; Okazaki, M.; Nakamura, A.; Kawai, S.; Sugimoto, M.; Matsumoto, Y.; Ohsugi, Y. Tocilizumab Inhibits Signal Transduction Mediated by Both mIL-6R and sIL-6R, but Not by the Receptors of Other Members of IL-6 Cytokine Family. *Int. Immunopharmacol.* **2005**, *5*, 1731–1740.